Objective Function for 4D Trajectory Optimization in Trajectory Based Operations

Octavian Thor Pleter[1] and Cristian Emil Constantinescu[2]

University Politehnica of Bucharest, 060042 Bucharest, Romania

and

Irina Beatrice Stefanescu[3]

Romanian Space Agency, 010362 Bucharest, Romania

In the future Air Traffic Management (ATM) implementations based on 4D trajectories, both the ATM problems (safe separation, sequencing for the best runway utilization) and the flight management problems (best fuel efficiency) may be solved together using a multidisciplinary optimization of all aircraft 4D trajectories. The paper presents advancements on 4D navigation based on an objective function for the optimization process, which effectively models the total costs and risks of air navigation. The resulted gate-to-gate 4D trajectories generated by a dynamic model flight simulator for the specific type of aircraft with the individual initial Flight Management System data are "flyable", and they present the best cost-risks trade-offs. The paper also reveals results on some simulated experiments using genetic algorithms to minimize the objective function presented.

Nomenclature

C = cost

C_D = coefficient of drag

---

[1] Associate Professor, Faculty of Aerospace Engineering, otp@brainbond.ro, Member AIAA.
[2] Associate Professor, Faculty of Aerospace Engineering, constantinescu_ce@yahoo.com
[3] Researcher, irina.stefanescu@rosa.ro

C_L	=	coefficient of lift
CAS	=	calibrated air speed
D	=	aerodynamic drag
D	=	potential damage as cost
DIS_{kZ}	=	horizontal (longitudinal or lateral) separation between aircraft k and the intruder Z
DIS_c^*	=	adjusted distance of flight in country c
E	=	number of functional engines
E_T	=	number of functional engines when taxi
$ELEV$	=	elevation of terrain above mean sea level
ETA	=	estimated time of arrival
ETD	=	estimated time of departure
ETE	=	estimated time en-route
ETT	=	estimated time of taxi before departure and after arrival
F	=	thrust
FF	=	fuel flow of one engine
FL	=	flight level (measured in hundreds of feet)
$FREM$	=	fuel left in the tanks at the destination gate
$FUEL$	=	fuel loaded in the tanks before departure
g	=	acceleration of gravity
GS	=	ground speed
H	=	z-axis barometric coordinate: height above mean sea level, flight level or altitude
H_{kZ}	=	barometric vertical separation between aircraft k and the intruder Z
k	=	flight management system sensitivity and damping parameters
K	=	normalization factor
L	=	aerodynamic lift
LAT	=	geodetic latitude
$LONG$	=	longitude
m	=	mass of aircraft

M	=	Mach number
MH	=	magnetic heading
MNE	=	maneuver envelope volume of an aircraft
$MTOM$	=	maximum take-off mass
N	=	number of aircraft using the system simultaneously at any given moment
OCA	=	obstacle clearance altitude above mean sea level
p	=	air pressure (static)
p	=	probability for the entire flight
P	=	unitary price or cost
POS	=	current position of the aircraft
R	=	risk
R	=	Earth radius in the spherical approximation
s	=	scale factor
S	=	aircraft reference area
t	=	time
T	=	air temperature
TAS	=	true air speed
TBO	=	trajectory-based operations
TC	=	true course (track)
TCR	=	total costs and risks
TH	=	true heading
$TRANSALT$	=	transition altitude
$URCh$	=	unitary rate charges for air traffic services
VAR	=	magnetic compass variance
VS	=	vertical air speed (rate of climb or descent)
VWV	=	vertical wind velocity (considered zero)
W	=	weight of aircraft
$\vec{W}$	=	wind vector

WD	=	wind direction (degrees "from" azimuth, with respect to true North)
WV	=	wind velocity
XTK	=	cross track distance
α	=	angle of attack
γ	=	trajectory path angle (zero vertical wind is assumed)
ε	=	tolerance
θ	=	pitch angle
Θ	=	characteristic time for risk exposure
ξ	=	atmospheric turbulence normalized index
π	=	hazard function of an undesired event
ρ	=	air density
σ	=	atmospheric relative density index
τ	=	angle between engine thrust vector and the fuselage reference line
ϕ	=	roll (bank) angle
χ	=	icing conditions normalized index

subscripts

0	=	at mean sea level, in international standard atmosphere conditions
a	=	arrival
avg	=	average
c	=	country airspace index
d	=	departure
D	=	significant arrival delays
F	=	fuel
G	=	terrain/ground/obstacles proximity
i	=	type of cost index

I	=	icing conditions
j	=	type of risk index
k	=	flight or aircraft index
M	=	maintenance
MS	=	maintenance needed as a consequence of the accumulated stress of the airframe
MSL	=	mean sea level
MT	=	maintenance needed as a consequence of the time of flight
N	=	navigation
NFZ	=	no fly zone
NN	=	navigation, crossing a noise protection volume
NO	=	navigation, overflight charges
NPV	=	noise protection volume
NR	=	navigation, avoiding no-fly zones
NU	=	navigation, avoiding turn-intensive routes
NV	=	navigation, avoiding occupying more flight levels at once
RVSM	=	reduced vertical separation minima
S	=	loss of separation
SAT	=	saturation
SCH	=	scheduled
TE	=	true East
TN	=	true North
TRG	=	targeted
W	=	weather (turbulence, wake turbulence, wind shear)
Z	=	intruder or wake vortex generator aircraft

I. Introduction

Trajectory-based operations (TBO) are now common grounds for both the American and the European future ATM implementations (NextGen and SESAR). They assume that each aircraft flies an agreed 3D or 4D

trajectory within certain accuracy limits, or that it flies most of the time within a published or pre-calculated cylindrical 3D tube (Required Navigation Performance). Given the accuracy limits, each trajectory is calculated as to be safely separated from the others. Thus, the current communication based control system will be made redundant.

The 4D TBO represents a breakthrough for both air traffic capacity and operational safety. Moreover, trajectory based operations will allow the aircraft to fly optimized routes and flight profiles, making the best use of tailwinds (or the best avoidance of headwinds) [1]. Real-time weather avoidance and noise abatement will be among other features of the new system, due to be operational in the next decade. In [2] the authors advanced a gate-to-gate 4D trajectory system, where the trajectory of each aircraft is not only safely separated from the others, but it is also an optimal trajectory in terms of costs and risks.

There are two mutually exclusive options for the future ATM system: (a) a "centric" concept, in which the system calculates all the 4D trajectories in a large area, and updates them in real time, or (b) a "free flight" concept, with independent and egoist users, trying to find their individual best ways to their destinations [3]. Trajectory based operations are required in both cases.

This paper focuses on a comprehensive objective function for a multidisciplinary optimization of the 4D trajectories in the framework of the variant (a). The authors trust this as the better option of the two, in terms of fuel economy, carbon emissions, safety, noise pollution, runway capacity, air traffic capacity. The total costs and risks approach seems to be an appropriate tool for the 4D trajectory optimization problem, which is expected to solve simultaneously both the flight and the traffic management problems [4].

To implement 4D TBO, two conditions must be met: (1) a dependable broadband air-to-ground data link capability must be operational, for real-time exchange of 4D trajectories between all aircraft and the ground air traffic control center network; (2) the flight management system (FMS) of each aircraft must be capable of 4DT following, within the required accuracy margin. This function is also known as Precision Trajectory Control[4]. The FMS should speed up the aircraft when the slightest delay occurs, or slow it down at the slightest advance versus the schedule, similar to the subliminal control [5]. The reason for this requirement is the need of using the landing runway (a critical resource of the entire ATM system) at reasonable capacity. The 4D trajectories of all aircraft will

---

[4] Current FMS are capable of just 2D to almost 3D trajectory following, within a large margin, but in the 4D TBO concept, the accuracy and the fourth dimension (time) capability are essential.

be automatically sequenced, and errors as small as seconds could threat the longitudinal separation in the final approach queue.

Although the current visions for the future ATM system share the 4D TBO concept tools, there are at least two distinct views of the matter. The most common view limits itself to ATM, attempting to solve just this problem [3], [6]. This view is justified by the urgency of solving this problem in the perspective of the air traffic increase. The second view, which the authors share, assumes the same tools, but takes advantage of them to an extent beyond the ATM problem [7], [8].

In a 4D TBO airspace environment, optimized trajectories may be easily implemented, thus improving costs and safety, reducing emissions and helping with reducing the noise of aircraft operations. As long as the 4D trajectories are generated on ground, they may be optimized together, allowing for the lowest costs and risks at any given moment, for the whole air traffic system of a large area (e.g. North America or Europe).

The 4D trajectories are not sequences of simple straight legs, turns, climbs and descents with time marks, as they appear. They are paths, which a certain aircraft is actually capable of flying, in certain load and performance conditions, under certain weather conditions and other limitations. They must be "flyable" 4D trajectories. If weather or performance conditions change (e.g. wind is not as forecasted, or there is an engine failure), current 4D trajectories may not be achievable, and therefore new ones have to be calculated by the ground center, and exchanged over the data link, to be further flown.

Although partial flight optimization concepts are in circulation, like the continuous descent approach [9], the authors believe that a gate-to-gate or complete flight optimization is more effective. The ground movement segments are very important for safety reasons, and in fact generate most delays starting from departure. It is possible to compensate for these delays in flight, but the stability of the air traffic system is improved with the gate-to-gate concept, as well as the safety of aircraft operations. The runways will remain the critical section of the air traffic system for years to come, making thus efficient use a critical objective.

This paper advances a gate-to-gate 4D trajectories multidisciplinary optimization method, by an adequate choice of the objective function, since as in any optimization problem, an uninspired choice of the objective function may lead to surprising results. In multidisciplinary optimization problems, an aggregate objective function is needed. This cost function is made of partial objective functions, which individually address every point of view, or discipline pertaining to the problem in question [10]. The balance of these components in the aggregate function is

usually adjusted by weight multipliers. As for constraints, Lagrange multipliers may be used, but sizing them may also be critical. For the trajectory optimization problem the authors developed a method to avoid arbitrary multipliers, for both the components and the constraints. The method advanced in [2] and [11] is designed to bring all the factors influencing the flight trajectory down to costs (in monetary terms). The currency unit is a natural common objective scale unit for all costs. Moreover, the authors decided to replace constraints with "risks". A risk is the cost of the potential damage multiplied with the probability of occurrence. Thus, the risks are expressed in monetary terms too. Our objective function is the Total Costs and Risks (TCR) for all aircraft trajectories in a given area, over a 3 to 12 hours horizon, due to accuracy of weather prediction and other operational factors.

For reasons explained in [12], the co-ordinate system used for trajectory calculations is the baro-geodetic (BGCS), with the geodetic latitude and longitude coordinates for horizontal position, and the barometric flight level, or altitude, as the vertical dimension.

To make sure that the 4D trajectories are "flyable", they are generated by an accurate flight simulator in real-time weather and operational conditions, and based on a 7th order dynamic model of the aircraft comprising of airframe with control surfaces, and a model of the aircraft engines. Thus, candidate 4D trajectories are slightly adjusted to become "flyable" 4D trajectories.

II.   The Total Costs and Risks Model

There are two misconceptions the authors needed to overcome before advancing to a functional model for air trajectory optimization: the total safety and the total efficiency.

(I) The first misconception was inspired by the ATC providers. They usually claim that "safety is everything that matters to us". When optimizing the performance of an ATM system, they would try to maximize safety expressed as a functional. A conflicting traffic scenario may be solved in a variety of different ways, out of which some are wasteful with the time (fuel) resources of the participants, some are economic for some participants, and some are economic for others. These solutions may be ranked by the total additional costs incurred by the solution chosen by the air traffic controller, but most ATC providers need there to be no occurrences of separation conflicts, and therefore do not discriminate further, between economic and wasteful solutions. The flaw of this approach is obvious: the safety function has its maximum at infinity, and the costs associated with infinite safety are also infinite. Practical ATM should be cost-effective, relying on a six-sigma approach (3.4 defects per million), with a

fault-tolerant system design (a safety net in place to capture the 3.4 defects), as opposed to maximum or infinite safety.

(II) At the opposite end of the scale there is the idea of total efficiency, the concept to minimize costs absolutely. It is usually attributed to airline operators. In their experiments with cost minimization functions, the authors often ended up with non safe trajectories. Indeed, minimizing costs usually leads to significant risks. For instance, an aircraft loaded with just enough fuel to touch down and to taxi to the gate will be the least expensive solution, as compared to an aircraft carrying a considerable fuel reserve, which adds to the weight. In terms of safety though, minimizing costs in such a manner would put the flight to an irrational risk.

The proposed Total Costs and Risks (TCR) model is a trade-off between safety and cost effectiveness. The objective function adds up both all costs influenced by the trajectory, and all risks incurred by the navigation

Figure 1. Trajectory optimization process.

process. For this purpose, costs and risks have to be additive and equally scaled. The word "total" has more than one significance: a) the term gathers "all" predictable costs and risks; b) these are estimated for the "entire" duration of the flight (gate-to-gate); c) the function is computed for "all" the aircraft flying in a wider area (TBO area), to ensure the separations.

The optimal 4D trajectory for each aircraft k may be computed by minimizing a TCR objective function:

$$TCR_k = \sum_i C_{i,k} + \sum_j R_{j,k} = \sum_i C_{i,k} + \sum_j p_j D_{j,k} = \min \qquad (1)$$

The costs and risks of a given solution to the 4D trajectory optimization problem for a single flight k, expressed in currency units (e.g. €), which depend on the 4D trajectory, are integrated over the entire flight. Damages are maximal costs of the possible damage arising from incidents or accidents caused by a bad choice of the 4D trajectory. The probabilities for the undesired events to occur are function of the 4D trajectory separation from other

trajectories, from terrain and obstacles, from dangerous weather phenomena, and from other operational hazards. The probabilities are computed [13] over the entire flight as integral functions of the instantaneous hazard functions π_j, as follows:

$$p_j = 1 - e^{-\int \pi_j dt} \tag{2}$$
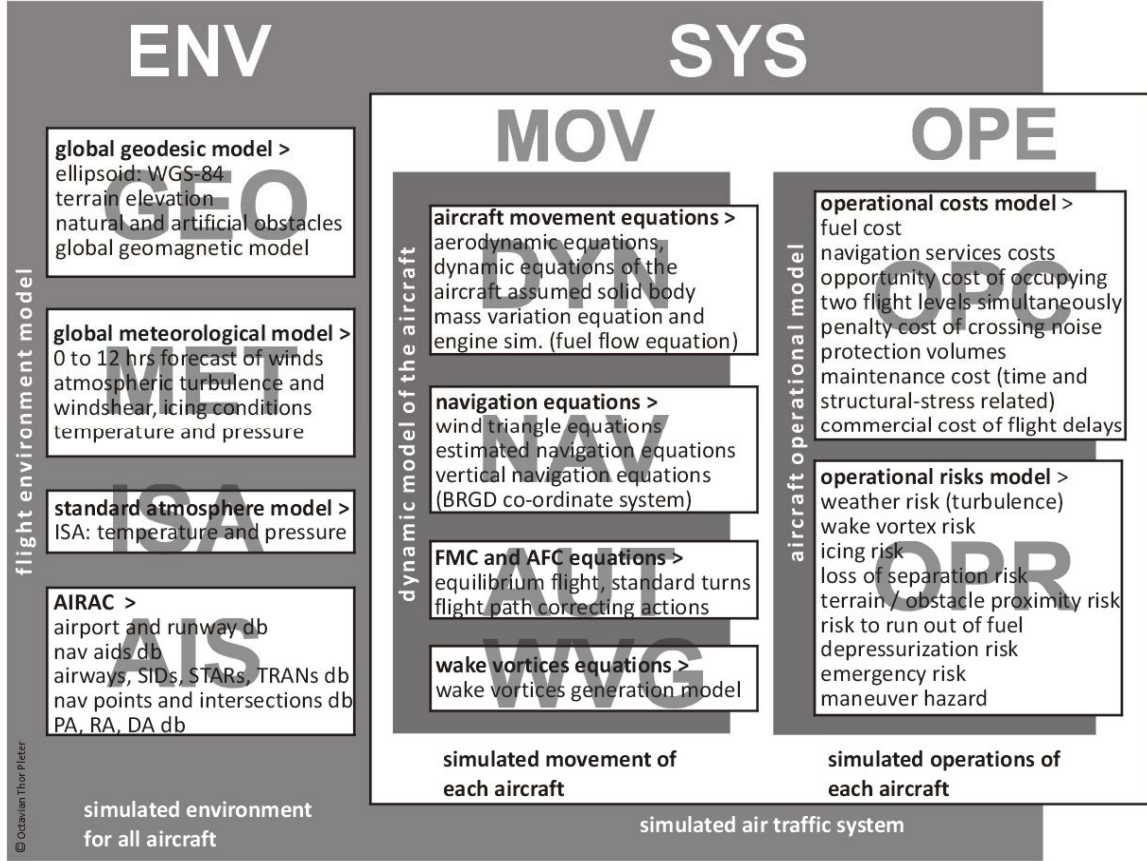
Figure 2. Simulator used for optimizations.

In a network-centric air transport system, all 4D trajectories flown at any given moment need to be safely separated from the computing phase. For this reason, the optimization process (see Figure 1) will include simultaneously all the flights due within the given TBO airspace. Before validating and uploading the optimized 4D trajectories to the user aircraft, the ground computers will minimize the TCR of all flights:

$$TCR = \sum_k TCR_k = \min \tag{3}$$

Figure 2 shows an analytical representation of the simulator used in the optimization process.

III. Trajectory-dependant Costs and Risks

The aircraft operational model consists of algorithms, which evaluate every foreseeable cost and risks of each flight, allowing the calculation of the aggregate TCR objective function for each traffic management solution. The optimization process iterates until an adequate suboptimal solution to the ATM problem is reached. The ideal optimal solution is not practical, due to calculus complexity and the optimization method (e.g. the genetic algorithms have no criterion to end the optimization process).

In this section, each cost and risk is discussed. (Note that some are presented without a mathematical support, since they are not yet validated through tests, or the relevant research work is still in progress). The numerical application addressed in this paper ignores those factors. (Their presence is indicative of our future intentions, and perhaps promising of new lines of research).

A. Fuel cost

The fuel cost C_F is the most significant cost of the flight and it heavily depends on the 4D trajectory chosen:

$$C_F = P_F \left(E_T \int_{ETT} FF(t) \cdot dt + E \int_{ETD}^{ETA} FF(t) \cdot dt \right) \tag{4}$$

To evaluate the instantaneous fuel flow, the authors identified a non-linear model of an engine from data stored in the digital flight data recorder (DFDR), which is illustrated in Figure 3. Whereas other dynamic variables depend on the type of aircraft, the engine model presents significant variations from one airframe to the other, moreover the same engine changes fuel flow characteristics during its operational life. The engine model is used to evaluate the instant fuel flow (the $FF(t)$ function in Eqs. 4,5), which depends on the required thrust. Thrust is an estimated variable determined from the current weight of the aircraft mg, true air temperature TAT and barometric height H (in the real atmosphere), corrected air speed CAS and its derivative $\overset{\circ}{CAS}$, and the vertical speed VS. The approximation function (Eq. 5 with the coefficients in Table 1) fits well the fuel flow of the real aircraft, with an integrated error between the simulator and the real aircraft of under 0.01% over a recorded 3 hours flight.

$$FF(t) = a_{01} \prod_{i=1}^{6} \left(a_{i1} \, \text{sgn}(x_i) \sqrt{|x_i|} + 1 + a_{i2}x_i + a_{i3}x_i^2 \right) \qquad (5)$$

The fuel cost minimization alone leads to: a) the *brachistochrone* route (maximum tailwind or minimum headwind component along the entire cruise) [1], b) the optimized flight profile, with c) the economic cruise speed. The optimized flight profile is made of a steep climb at the beginning, followed by a gradually softer climb until the mid point (the solid line in Figure 4). There is no level flight, and the top of climb is very close to the top of descent. The optimal descent profile is also very long, with a slight descent at first, followed by an economic continuous descent, with idle engines. Given the flight levels scheme in use today, the optimal flight profile has little practical value because the aircraft keeps a block of more flight levels occupied almost the whole cruise, inflicting a heavy penalty upon the airways capacity. There is little gain from the long quasi-level cruise flight profile, so under the circumstances of the current ATM practices, the cruise profile needs to be flattened to level flight (Figure 4, dotted line) by introducing an artificial navigation services penalty cost (see B below). In the future ATM environment
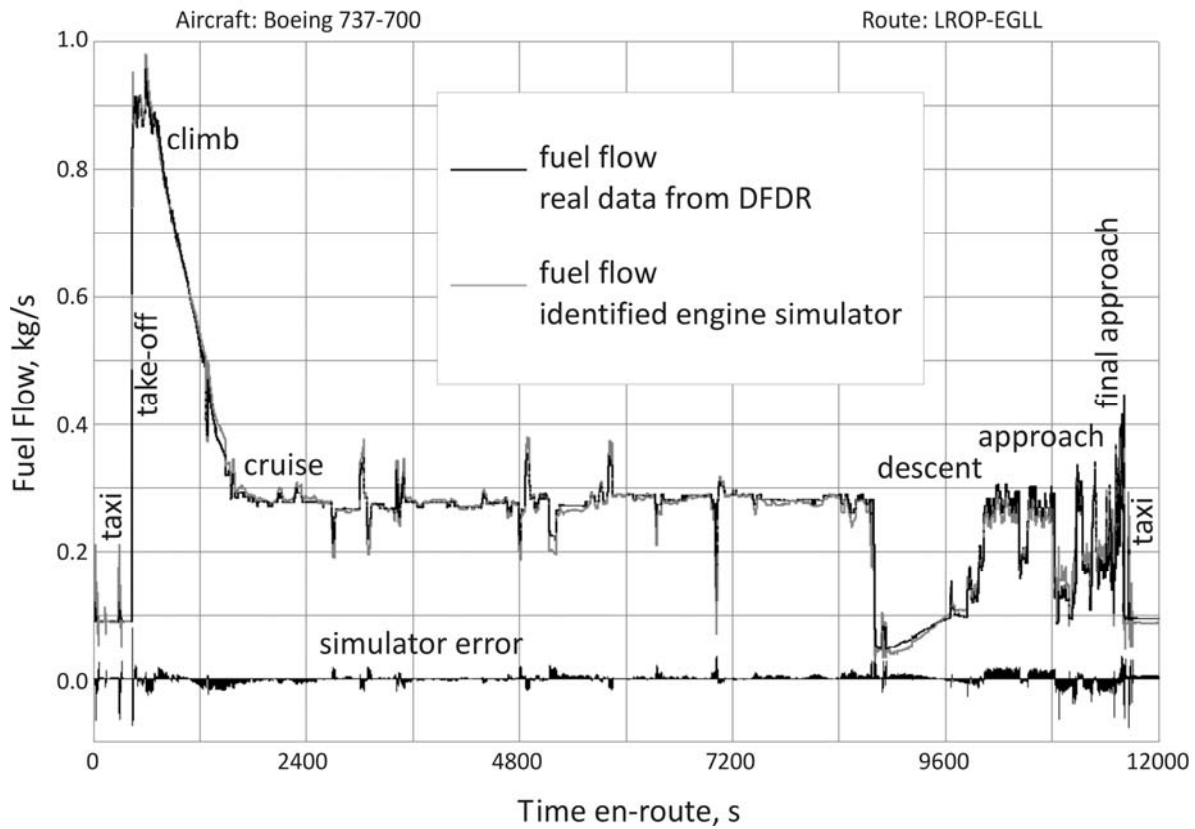
Figure 3. **Identification of an engine model.**

12

though, the need to cruise at a constant flight level would not matter as much as today, and probably, such a precaution would be eliminated.
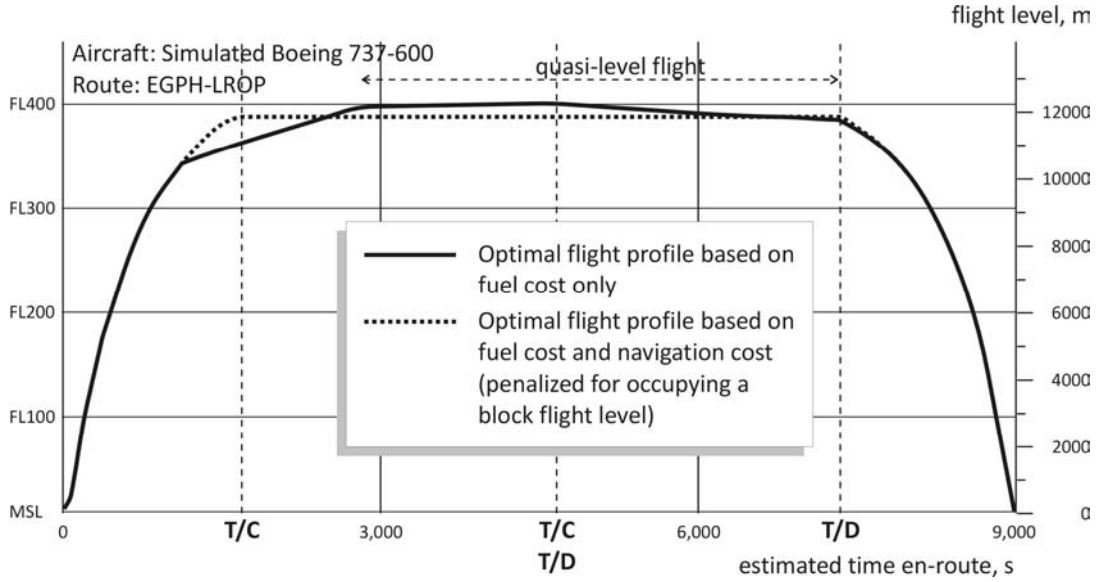
Figure 4. Experimental optimal flight profile.

B. **Navigation costs**

Navigation costs C_N include the fees charged by the air navigation service providers C_{NO}, and the following artificial costs, aimed at influencing the trajectory: C_{NV} (the level flight enforcement penalty), C_{NR} (the no-fly zone enforcement penalty), and C_{NN} (the noise reduction enforcement penalty). The airport fees C_{NA} are not included in C_N since they are unavoidable and invariant to the solution of the trajectory optimization problem, providing that the aerodrome of departure and the aerodrome of arrival are given.

In Europe there are very different costs (in a range of 1 to 4) for over flying one state or another. Although the overflight fees may have a marginal impact on most solutions to the 4D trajectory optimization problem, they belong to the objective function, using the formula provided by Eurocontrol [14] used when charging the users of the airspace:

$$C_{NO} = \sum_{c=1}^{N} \left(\sqrt{\frac{MTOM}{MTOM_{avg}}} \cdot \frac{DIS_c^*}{DIS_{avg}} \cdot URCh_c \right) \tag{6}$$

$$DIS_c^* = \int_{POS \in c} GS(t) \cdot dt - DIS_d \big|_{c=1} - DIS_a \big|_{c=N} \tag{7}$$

13

The unitary rate of charge published by Eurocontrol for every country c [15] will force the resulted 4D trajectory to over fly the expensive countries as little as practicable. In the future European ATM environment, uniformity of the navigation charges is expected, so the relevance of this cost in the objective function will be probably lost.

Two of the artificial navigation costs (C_{NV} and C_{NU}) penalize unwanted behaviors of the 4D trajectory: a) the quasi-level flight of the optimal profile (see A.), and b) avoid turn-intensive routes, which for instance make loops, slowing down the optimization process. The other two (C_{NR} and C_{NN}) allow for: a) the enforcement of the no-fly zones, generating the trajectory that avoids various types of operational restrictions (prohibited areas, restricted areas etc.), and b) the implementation of two important concepts for the future of air navigation: the *flexibly restricted airspace*, and the *noise protection area*.

To prevent the quasi-level flight yielded by the optimized trajectory (Figure 4) and to enforce an efficient use of the airspace, C_{NV} was introduced. This cost is zero below the transition altitude and in level flight at any fixed valid standard flight level (FL320, FL330 etc.), according to the reduced vertical separation minima (RVSM) scheme [16]. The cost C_{NV} is not zero in level flight at any intermediary or opposite flight level (e.g. FL324). This cost is proportional with the time en-route in the non zero condition.

Eqs. 8-9 implement the RVSM logic.

$$C_{NV} = P_{NV} \int_{ETD}^{ETA} \left(\left(\sin\left(2\pi \left(FL(t) - a_H + a_E a_V / 2 \right) / a_V \right) + 1 \right) / 2 \right) \cdot dt \tag{8}$$

$$a_V = \begin{cases} 20 & \Leftarrow FL(t) \le 410 \\ 40 & \Leftarrow FL(t) > 410 \end{cases} \quad a_H = \begin{cases} 5 & \Leftarrow FL(t) \le 410 \\ 0 & \Leftarrow FL(t) > 410 \end{cases} \quad a_E = \begin{cases} 1 & \Leftarrow 0 \le MH(t) < 180 \\ 0 & \Leftarrow 180 \le MH(t) < 360 \end{cases} \tag{9}$$

C_{NU} has no other purpose than speeding up the algorithm in the early stages, and no other side-effect on the final solution. Experiments indicated that the weight of C_{NU} in the *TCR* becomes zero during the optimization process. A unitary price P_{NU} per radian of turn is charged (see the numerical values of the unitary prices in Table 2), and it is calculated as the cost of the cumulated course changes during the entire flight (Eq. 10). Consequently, the routes with many large turns and loops are discarded earlier as unpromising, and the straight or more direct ones are kept.

$$C_{NU} = P_{NU} \int_{ETD}^{ETA} \left| \overset{\circ}{TH}(t) \right| \cdot dt \tag{10}$$

The AIS database of the simulator (see the AIS block in Figure 2) includes permanent or temporary *no-fly zones*, volumes of airspace which must be avoided by all aircraft. The optimizer manages this through this high penalty cost C_{NR} for the slightest intrusion in such a restricted volume:

$$C_{NR} = P_{NR} \int_{ETD}^{ETA} \Delta_{NR}(t) \cdot dt \tag{11}$$

$$\Delta_{NR}(t) = \left(POS(t) \in POS_{NFZ}\right) \wedge \left(H(t) \leq H_{NFZ}\right) \tag{12}$$

The new TBO-specific concepts, the *flexibly-restricted airspace*, and the *noise protection volume*, allow a flexible avoidance of a certain volume of airspace. These procedures are required for operational reasons, or on noise and emissions protection grounds. A rigid restriction (e.g. a no-fly zone) is known to concentrate traffic tensions at the restricted area boundary, enhancing the risk of conflicts at the boundary. To mitigate this risk, the advocated approach allows for a few of the trajectories to cross the border into the restricted area, at peak traffic loads, hereby easing a safety critical complex traffic situation. The *flexibly-restricted airspace* and the *noise protection volume* may be implemented with the same cost tool as the *no-fly zone* (Eqs. 11-12), but using a different, much lower, P_{NR}:

$$C_{NN} = P_{NN} \int_{ETD}^{ETA} \Delta_{NN}(t) \cdot dt \tag{13}$$

$$\Delta_{NN}(t) = \left(POS(t) \in POS_{NPV}\right) \wedge \left(H(t) \leq H_{NPV}\right) \tag{14}$$

C. Maintenance costs

Maintenance costs C_M include two components, which both depend on the chosen trajectory. One cost is proportional to the time of flight, and the other one is proportional to the stress of the airframe during the flight, both integrated over the duration of the flight:

$$C_M = P_{MT}\left(ETE + ETT\right) + P_{MS} \int_{ETD}^{ETA} \xi\left(POS(t)\right) \cdot dt \tag{15}$$

15

As a proxy for the airframe stress, the turbulence index was considered (see E). The unitary prices may be calculated from the financial statements and the flight records of each aircraft operator. Table 2 represents the values considered in the numerical experiments.

D. Cost of delays

Due to traffic, weather, or operational causes, the estimated time of flight between take-off and landing (*ETE*) could face extensions. These are penalized by both the cost of fuel and the first term in the cost of maintenance, but if the delay is over a threshold ETE_D beyond the scheduled estimated time of arrival for scheduled passenger services ETA_{SCH}, some additional commercial costs C_D could be expected. Their growth is non-linear, and has the form presented in Figure 5, based on time evolution captured in Eq. 16.
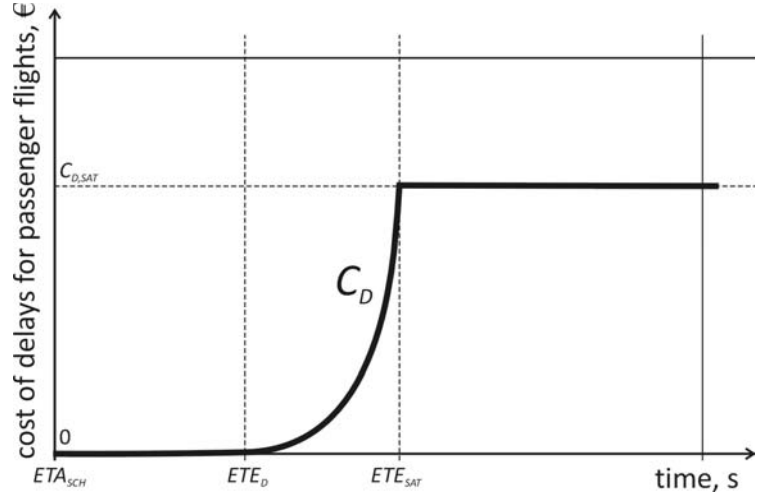
Figure 5. Cost of delays of passenger flights.

$$J = P_D \cdot e^{\left(ETA - ETA_{SCH} - ETE_D\right)/K_D}$$

(16)

$$C_D = \begin{cases} 0 & \Leftarrow & ETA - ETA_{SCH} < ETE_D \\ J & \Leftarrow & \left(ETA - ETA_{SCH} \geq ETE_D\right) \wedge \left(J \leq C_{D,SAT}\right) \\ C_{D,SAT} & \Leftarrow & J > C_{D,SAT} \end{cases}$$

(17)

The effect of including this non-linear cost in the objective function is to prioritize for those scheduled passenger services threatened by delays over $ETA_{SCH} + ETE_D$.

E. Weather risk

The weather risk R_W is used in the objective function as a tool for finding the best trade-off between a solution to fly through bad weather and one to fly around it. The potential damage captured by the weather risk D_W is the loss of the aircraft, and consequential loss of lifes of the passengers and the crew. This parameter must be selected as being

16

much larger than the current operational expenses (see D in Table 2), so that under no circumstance could a trajectory be issued with a probability of such a loss. This cost acts like a constraint, and enforces safe and prudent trajectory planning. For its purpose in the optimization process, accuracy for the values of these D parameters is not required.

Table 2.   Unitary prices and other financial parameters used in optimization function

parameter	significance and use	units	typical value
$C_{D,SAT}$	passenger aircraft delay of arrival saturated cost	€	3,000
D	potential loss of the aircraft cost	€	500,000,000
P_D	typical cost a carrier is charged due to a delay of a scheduled passenger service	€/s	1,000/3,600
P_F	aircraft fuel unitary price	€/kg	0.93
P_{MS}	maintenance price as a consequence of the accumulated stress of the airframe (e.g. flight in turbulent atmosphere)	€/s	10
P_{MT}	maintenance price needed as a consequence of the flight time	€/s	0.15
P_{NN}	unitary penalty cost for intruding a noise protection volume	€/s	1,000/300
P_{NR}	unitary penalty cost for intruding a no-fly zone	€/s	1,000
P_{NU}	unitary penalty cost for turns along the route	€/rad	1,000/(2π)
P_{NV}	unitary opportunity cost of the air services provider if an aircraft occupies more than a single standard valid flight level according to the RVSM scheme	€/s	100/3,600

The probability of the weather risk p_W is the accumulated hazard function π_W, which is considered equivalent to the local turbulence index encountered $\xi(POS(t))$ along the entire flight:

$$p_W = 1 - e^{-\int_{ETD}^{ETA} \pi_W(t) \cdot dt} \tag{18}$$

$$\pi_W = \xi\big(POS(t), CAS(t), M(t)\big) / \Theta_W \tag{19}$$

The hazard function is proportional to the forecasted local turbulence index along the route ξ. This index is published by the global weather providers (up to a day in advance), or downloaded from the aircraft already in flight. The index ξ is a function of the aircraft current position in the simulated environment. It has a normalized value, varying from 0 (no atmospheric turbulence) to 1 (extremely severe turbulence). The ξ variable accepts other two distinct meanings: a) the destabilizing effect of the wake vortices generated in the current position by surrounding traffic (using a wake vortices generation model), and b) the windshear, experienced during final

approach and departure. All three phenomena could share the same index cumulatively, since they are translated into the same avoidance rule for the trajectory optimizer.

The turbulence hazard also depends on the speed of the aircraft (*CAS* or *M*, depending on the flight phase), and it is aggravated when the aircraft flies at the envelope limits, (i.e. at the best forward speed).

Note that all hazard functions require a time characteristic parameter, which depends on the phenomenon as presented in Table 3.

Table 3. **Characteristic time parameter used in optimization**

parameter	significance and use	units	used value
Θ_G	characteristic time for terrain/ground/ obstacle risk exposure	s	60
Θ_I	characteristic time for icing risk exposure	s	200
Θ_S	characteristic time for separation risk exposure	s	30
Θ_W	characteristic time for weather risk exposure	s	100

The term R_W in the objective function will enforce weather avoidance, with preference to those routes and flight levels clear of turbulence. It will also enforce avoidance of the wake vortices generated by other traffic, and windshear.

F. Icing risk

The icing risk R_I is used in the objective function as a tool for finding the best trade-off between a solution to fly directly through a volume of atmosphere with icing conditions and a solution to go around, either vertically or horizontally. All potential damages *D* were considered equal to the worst scenario (i.e. an accident). The Eqs. 20-21 are similar to the previous ones, with the local icing conditions index χ, also reported by the weather providers and/or in flight.

$$p_I = 1 - e^{-\int_{ETD}^{ETA} \pi_I(t) \cdot dt} \tag{20}$$

$$\pi_I(t) = \chi(POS(t))/\Theta_I \tag{21}$$

G. Loss of separation risk

The loss of separation risk R_S is used in the objective function as a tool for finding the best trade-off between a solution to increase traffic capacity through a reduction of separation margins and a solution requiring separated aircraft by a large margin. The loss of separation hazard function between every pair of flights *k* and *Z* at any

18

moment is a function π_S, taking a form of an inverse exponential (see Figure 6) with the instantaneous horizontal distance DIS_{kZ} between the two aircraft, or zero if the applicable vertical separation $VSEP$ is equal or exceeded by a small margin ε_H versus the vertical separation H_{kZ}:

$$p_S = 1 - e^{-\int_{ETD}^{ETA}\left(\sum_{\substack{Z=1 \\ Z\neq k}}^{N}\pi_{S,Z}(t)\right)\cdot dt} \tag{22}$$

$$\pi_{S,Z}(t) = \left(1 - \operatorname{sgn}\left(H_{kZ}(t) - VSEP(t) + 2\varepsilon_H\right)\right) / \left(2e^{DIS_{kZ}(t)/K_S} \cdot \Theta_S\right) \tag{23}$$

$$DIS_{kZ}(t) = R\sqrt{\left(LAT_Z(t) - LAT_k(t)\right)^2 + \left(LONG_Z(t) - LONG_k(t)\right)^2\left(\cos^2\left(\frac{LAT_k(t) + LAT_Z(t)}{2}\right)\right)} \tag{24}$$

$$H_{kZ}(t) = \left|H_Z(t) - H_k(t)\right| \tag{25}$$

This logic corresponds to the current practice employed in air traffic control. The vertical separation in RVSM airspace is 304.8 m (1,000 ft) below FL410, and 609.6 m (2,000 ft) above FL410, except when either H_k or H_Z are around the transition altitude (*TRANSALT*). In this critical case, the vertical separation should be significantly larger, to mitigate the risk of loss of actual separation due to the possible altimeter-setting discrepancy between two adjacent aircraft, possible human error, or technical fault in the altimeter-setting. The loss of separation risk is significant only when the two aircraft come relatively close, and thus the
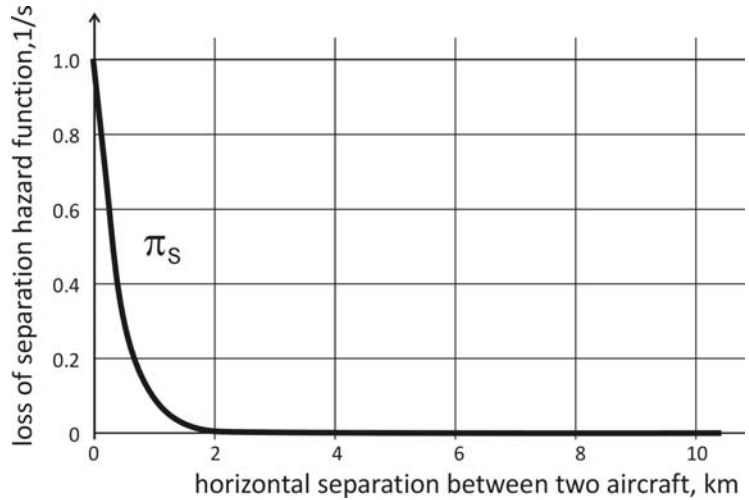
Figure 6. The loss of separation hazard function.

approximation used in Eq. 24 is justified. The potential damage of the loss of separation risk D_S is D. The loss of separation risk probability p_S of each trajectory is calculated in a loop, considering all other aircraft as intruders, and adding up the calculated hazard functions.

H. Terrain proximity risk

The terrain (ground or obstacles) proximity risk R_G is used in the objective function as a tool to find the best trade-off between a solution with an early turn after take-off, low path angle climb, low clearance margin from obstacles, as opposed to a solution with very steep climb, long straight departure, and increased obstacle clearance margin. The impact of R_G upon the optimization process is to ensure that all trajectories stay away from the obstacles on the ground,
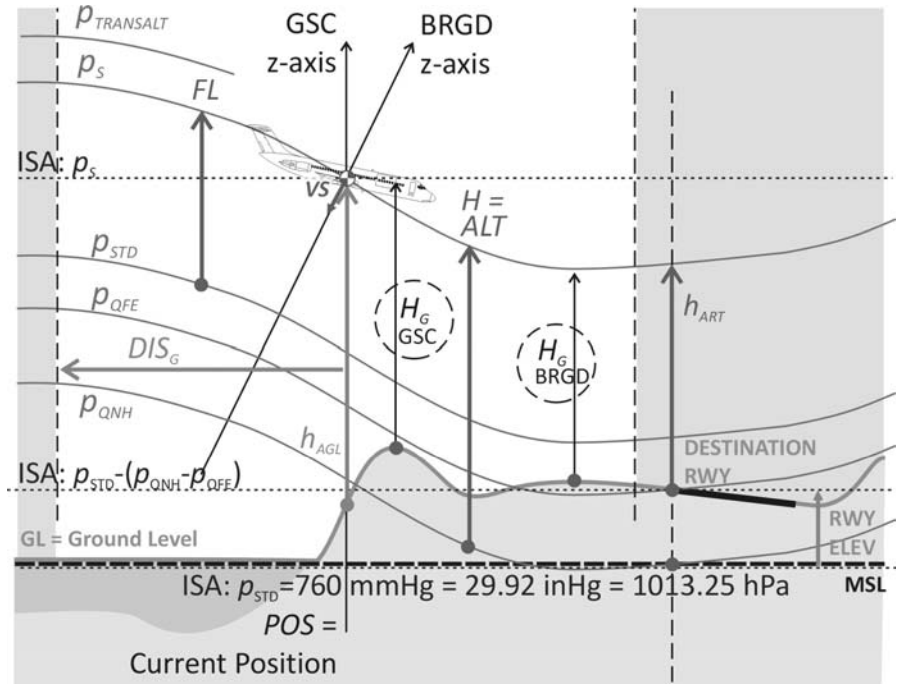
Figure 7. The greatest terrain threat H_G.

reducing the probability of controlled flight into terrain (CFIT) accidents (i.e. when a controllable aircraft is flown into the ground, water or ground obstacles). A special role is played by R_G in the case of departures and approaches in mountainous areas, or close to cities with high buildings. Shaping the trajectory around these threats means favoring early climb and late descent, as in the continuous descent approach. The terrain proximity risk hazard function π_G is an inverse exponential of the greatest threat H_G. This is the vertical distance between the isobaric surface of the aircraft, and the isobaric surface of the tallest terrain elevation or obstacle altitude, whichever is greater, in a circular area centered on the aircraft, with a radius of DIS_G (Eq. 26). As illustrated in Figure 7, in the real atmosphere this greatest threat could be different when defined in the *geodetic spherical coordinates* system and the *baro-geodetic system* (compare H_G GSC and H_G BRGD in Figure 7; although the former is higher geometrically, the later comes closer to the aircraft in level flight, due to the drop in the QNH pressure over the lower hill). In BRGD the *z* axis is always normal to the local isobaric surface. Considering that level flight maintains the isobaric surface and not the horizontal, the BRGD representation is more accurate.

The horizontal distance within DIS_G is not accounted in the hazard function (see Eq. 27), since a positioning error of the navigation system, or a loss of situational awareness of the crew may easily absorb this separation (as some past occurrences demonstrated [2]).

Table 4. Other parameters and constants used in optimization

parameter	significance and use	units	typical value
DIS_a	distance offset at arrival (used for C_{NO})	m	20,000
DIS_{avg}	distance constant used for C_{NO}	m	100,000
DIS_d	distance offset at departure (used for C_{NO})	m	20,000
DIS_G	horizontal distance radius from the current position where the algorithm looks for terrain or obstacle threats	m	3,700
ETE_D	maximum delay of arrival for a passenger aircraft without penalty costs for the carrier	s	1,200
ETE_{SAT}	saturated delay of arrival for a passenger aircraft	s	4,800
$FREM_{TRG}$	reasonable fuel reserve left at the destination gate (for 15-30 minutes of cruise flight); the targeted average fuel left in the tanks at the destination gate	kg	500
$MTOM_{avg}$	mass constant used to calculate C_{NO}	kg	50,000
K_D	normalization coefficient for delays	s	3,600
K_G	normalization factor for the terrain risk	m	30
K_L	normalization factor for fuel reserve	kg	150
K_S	normalization factor for separation	m	370
R	approximate Earth radius	m	6,371,000
T_0	air temperature at mean sea level (in international standard atmosphere conditions)	K	288.16
T_{STR}	air temperature in the stratosphere (in international standard atmosphere conditions)	K	216.66
$TRANSALT$	transition altitude from QNH to STD altimeter setting	m	5,486 in the US; variable in Europe
$VSEP$	vertical separation minimum (RVSM is assumed)	m	610 above FL410; 305 below FL410; 1,524 if at least one aircraft is around $TRANSALT$
ε_H	semi-tolerance of vertical-separation loss	m	15

$$H_G(t) = \left| H_k(t) - \max_{DIS_k < DIS_G} (ELEV, OCA) \right| \qquad (26)$$

$$p_G = 1 - e^{-\int_{ETD}^{ETA} \pi_G(t) \cdot dt} \qquad (27)$$

$$\pi_G(t) = e^{-H_G(t)/K_G} / \Theta_G \qquad (28)$$

In order to evaluate R_G, the simulator includes a global geodesic model $ELEV = ELEV(LAT,LONG)$, and a global obstacles model $OCA = OCA(LAT,LONG)$, taking advantage of the databases currently in use for the enhanced

proximity warning systems. Since there are no local static pressure measurements at the obstacle positions, the isobaric surfaces are approximated by interpolation from the global meteorological model of the real atmosphere, forecasted for the time of flight: $p=p(LAT,LONG,t)$ and $T=T(LAT,LONG,t)$.

I. Low fuel risk

At peak traffic times, the trajectory optimizer will be forced to frequently update the trajectories, and to delay some of the flights. The critical air traffic resource remains the runway, and for that reason, apart from a tight sequencing of arrivals and departures, the optimizer will be left with no other option than to delay flights, in some cases right at departure. Obviously, a gate-to-gate 4D trajectory optimizer does much better in terms of minimizing the delays that the current system generates (e.g. by subliminally decreasing cruise speed, instead of spiraling the aircraft on holding stacks).

Delays are unavoidable in some crowded traffic situations, or in emergency situations. The foreseen problem that the optimizer for the whole traffic can experience is that it might incidentally penalize one individual flight too much. To avoid the consequences of such a hypothesis, the low fuel risk R_L was introduced. This is nil for the aircraft with a sufficient fuel reserve, and soars for an aircraft with low fuel margin for the rest of the flight.

$$p_L = \begin{cases} 0 & \Leftarrow & FREM \geq FREM_{TRG} \\ e^{-FREM/K_L} & \Leftarrow & FREM < FREM_{TRG} \end{cases} \tag{29}$$

$$FREM = FUEL - E_T \int_{ETT} FF(t) \cdot dt - E \int_{ETD}^{ETA} FF(t) \cdot dt \tag{30}$$

$FREM_{TRG}$ is a reasonable fuel reserve left at the destination gate (e.g. for 15-30 minutes of cruise flight), or the targeted average fuel left in the tanks at the destination gate. If the aircraft consumes its navigation reserve due to unexpected vectoring, weather avoidance, strong headwind or other reasons, R_L will prioritize it in the approach phase.

The rest of the risks discussed below are presented mainly to show the work in progress. Such risks will be quantified in a similar fashion and will represent future improvements of the objective function.

J. Depressurization risk

The depressurization risk is used in the objective function as a tool for finding the best trade-off between a solution requiring direct routes over high mountains, versus a solution to fly routes, which allow rapid descent in case of depressurization, to an altitude where there is no need for the oxygen masks. In high and wide mountainous regions (e.g. over the Himalayans), the minimum safe altitude is higher than the depressurized cabin maximum pressure altitude, making the emergency descent maneuver impossible (Figure 8). To avoid such a situation, the depressurization risk will minimize the time of flight over high mountains.
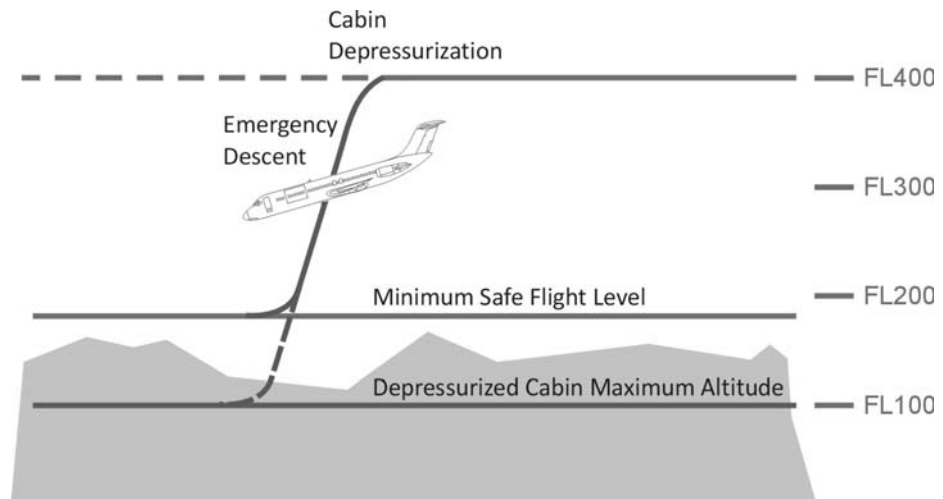
Figure 8. Depressurization risk.

K. Emergency risk

The emergency risk is used in the objective function as a tool to quantify the best trade-off between a solution requiring flying direct routes regardless of the airports suitable for emergency landing, versus a solution requiring flying routes, which allow emergency landing within reach. This term offers a 4D trajectory solution with a generalization of the ETOPS[5] concept.

L. Maneuver hazard risk

The maneuver hazard risk is used in the objective function for finding the best trade-off between a solution taking no precautions for unexpected maneuvers of another aircraft, and a prudent solution, allowing for additional time separation margin necessary to mitigate any intruder unexpected maneuvers. In a 4D TBO system, the maneuver hazard occurs when an aircraft becomes uncontrollable, or is not a user of the ATM system (airspace

---

[5] Extended-range Twin-engine Operational Performance Standards, an International Civil Aviation Organization (ICAO) rule permitting twin-engined commercial air transporters to fly routes that, at some points, are farther than 60 minutes flying time from an emergency airport, with one engine inoperative.

intruder), or is not flown any more under 4D FMS guidance for some reason. The appropriate response to such hazards would be to assume any offender possible maneuver within the envelope, and to prudentially divert all the traffic in close vicinity, modifying the 4D trajectories accordingly. Such a risk is considerable in a crowded TBO airspace, when one aircraft happens to escape its assigned trajectory.

The probability of the maneuver hazard risk p_M depends of the type of offender aircraft Z. The ATM network will need the following information on a continuous basis: the position, the ground speed and the offender type of aircraft. If the type of aircraft is not known, the most critical type must be assumed (the aircraft with the widest maneuver envelope). The maneuver envelope MNE_z is a volume around the aircraft Z, which includes all the possible trajectories within a certain time horizon of flight, from the steepest climb to the steepest dive, from the smallest radius left turn to the right turn, all in the range of the airspeeds the aircraft is capable of (see Figure 9).
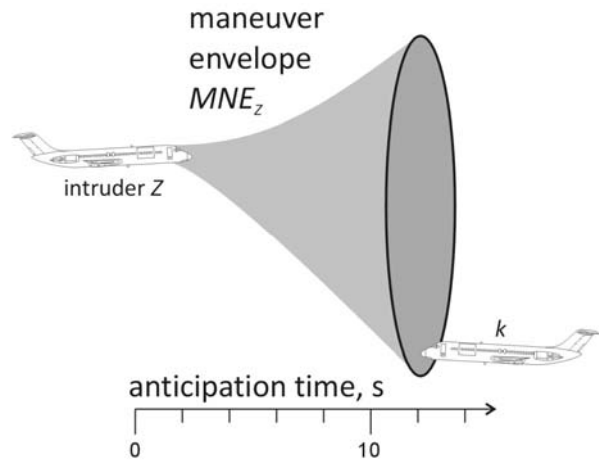
Figure 9. The maneuver hazard.

As in the previous cases, the potential damage of the maneuver hazard risk D_M is considerable lower than the complete loss of the aircraft. The reason for this is the probable action of a safety net, the traffic collision avoidance system.

IV. The Dynamic Aircraft Model

The simulator used in the numerical applications (Ch. 5) relies on a dynamic model presented in Eqs. 31-41, which includes the mass variation. Usually, kinematic models are used to address ATM problems, but a dynamic model seems more appropriate in this case, for three reasons: a) the gross mass at departure and the mass variation along the route are factors which matter in deciding which aircraft should climb, or descend in case of conflict, due to a influence on performance; b) in order to optimize the fuel consumption of each aircraft, the fuel flow calculated by the engine model (Eq. 5) is required; c) the trace is realistic in all types of maneuvers: turns, climbs, descents, which improves the reliability of the separation calculus. The differential system characterizing the aircraft model was reduced from 13th to 7th order, considering mass variation.

$$L = (\rho_0 / 2) CAS^2 \cdot S \cdot C_L(\alpha) \tag{31}$$

$$D = (\rho_0 / 2) CAS^2 \cdot S \cdot C_D(\alpha) \tag{32}$$

The $C_L(\alpha)$ and $C_D(\alpha)$ functions result from an algorithm based on data published in [17].

$$m \cdot TAS \cdot \overset{\circ}{\theta} = F \sin(\alpha + \tau) + L - \left(mg \cos\phi + m \cdot TAS \cdot \overset{\circ}{TH} \sin\phi \right) \cos\gamma \tag{33}$$

$$m \cdot \overset{\circ}{TAS} = F \cos(\alpha + \tau) - D - mg \sin\gamma \tag{34}$$

$$\overset{\circ}{TH} = g \cdot \tan\phi / (TAS \cdot \cos\gamma) \tag{35}$$

$$\overset{\circ}{m} = -E \cdot FF\left(mg, T, H, CAS, \overset{\circ}{CAS}, VS \right) \tag{36}$$

$$GS_{TN} = TAS \cos\gamma \sin(\pi/2 - TH) + WV \sin(3\pi/2 - WD) \tag{37}$$

$$GS_{TE} = TAS \cos\gamma \cos(\pi/2 - TH) + WV \cos(3\pi/2 - WD) \tag{38}$$

$$\overset{\circ}{LAT} = GS_{TN} / (R + H) \tag{39}$$

$$\overset{\circ}{LONG} = GS_{TE} / ((R + H)\cos LAT) \tag{40}$$

$$\overset{\circ}{H} = TAS \sin\gamma / \cos\alpha + VWV \tag{41}$$

International standard atmosphere is assumed. Finally, the whole flight is supposed to be equilibrium flight, in trim conditions and with all turns coordinated, permanently under flight management computer guidance, modeled with Eqs. 42-44, with the sensitivity parameters in Table 5:

$$\phi = k_\phi \max\left(\min(XTK, XTK_{SAT}), -XTK_{SAT} \right) - k_{TC} (TC - TC_{TRG}) \tag{42}$$

$$\overset{\circ}{\theta} = k_H \max\left(\min\left(H_{SAT}, H - H_{TRG}\right), -H_{SAT}\right) - k_\theta\left(\theta - \alpha\right) \tag{43}$$

$$\overset{\circ}{CAS} = k_{CAS}\left(CAS_{TRG} - CAS\right) \tag{44}$$

V. Numerical applications

The approach to test the objective function is in two steps: a) simulated numeric validation, by

Table 5. Parameters of the Flight Management Computer

parameter	significance and use	units	used value
k_θ	pitch control damping	-	0.21
k_H	pitch control sensitivity	rad/m	$9.76{\cdot}10^{-5}$
H_{SAT}	height saturation	m	304.2
k_ϕ	roll control damping	rad/m	$1.884{\cdot}10^{-5}$
k_{TC}	roll control sensitivity	-	0.5
XTK_{SAT}	cross track saturation	m	9,260
k_{CAS}	airspeed sensitivity	-	1/60

comparing the results with actual flights, as presented in the digital flight data recorder (DFDR) data; b) optimization of a single 4D trajectory of a real flight, contrasting the results with the actual flight. The purpose of the objective function is the simultaneous optimization of 4D trajectories of more aircraft, but in the test phase, such a problem would make validation difficult.

Although our concept addresses the whole gate-to-gate trajectory, the simulations in the cases below were limited to the flight phase. The simulator for the ground movement, and the database of the airport maps are under development.

To validate the simulator by comparing its results with the DFDR data, an individual aircraft was chosen (Boeing 737-78J,

Table 6. Results for a single flight optimization

flight	TCR (including fuel costs)	fuel costs
actual	-	€5,231
orthodrome	€8,904	€5,772
optimized with TCR	€5,964	€4,392

registered YR-BGI), for which these data were made available to the authors. Whereas the flight simulator is the same for all B737-700 Series, the instant fuel flow of the engine simulator depends on the individual aircraft, as the engines change slightly in their fuel consumption characteristics.

For actual flights of this aircraft, the weather conditions were recorded (i.e. the wind vector field at all flight levels, turbulence etc). For this purpose, the National Oceanic and Atmosphere Administration (NOAA) distribution system [18] was used. With this information, the flight in the same conditions was simulated, comparing the

simulated 4D trajectory with the actual one. The simulator emulates the real aircraft in real environment very well: For instance, a three hours flight was simulated with a H_∞ accuracy of 0.36% in distance and 0.63% in time.
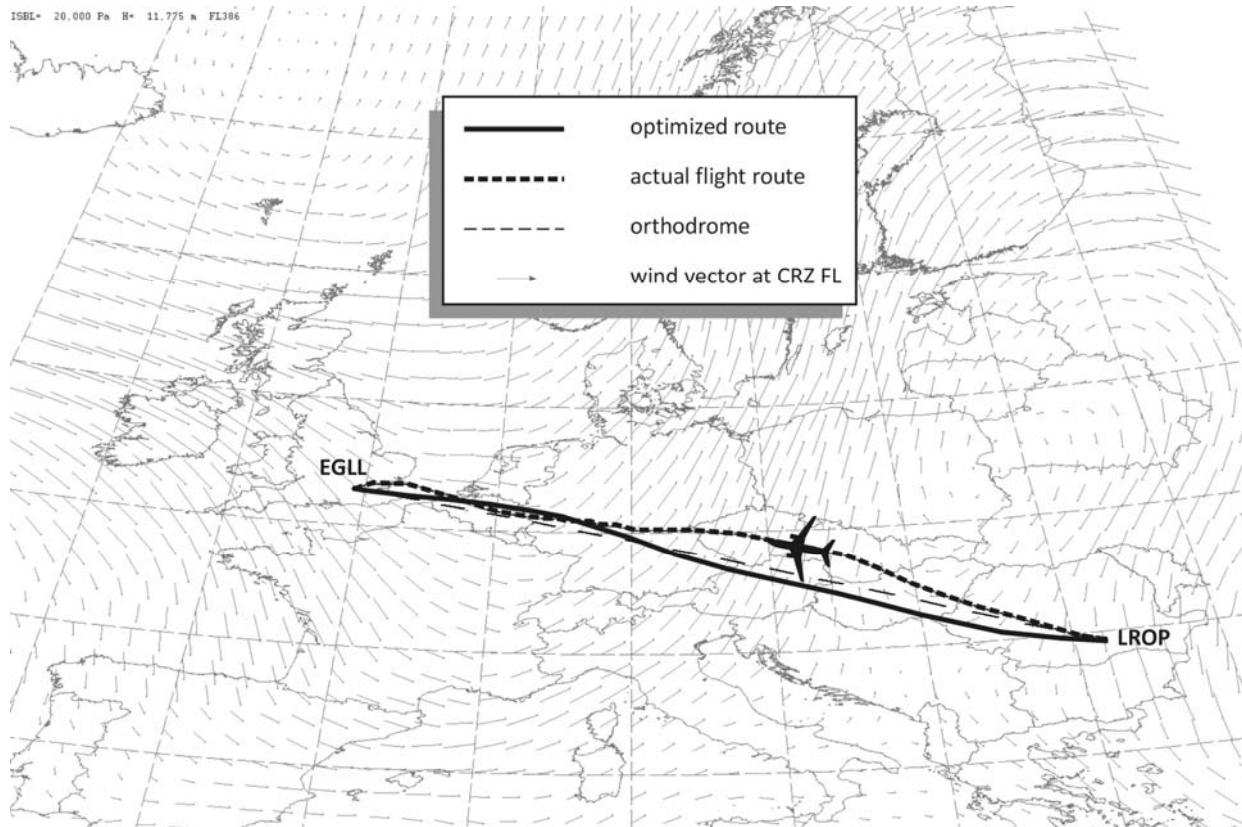
Figure 10. The optimized route, compared to the orthodrome, and to the actual flight route.

The second step was to use the simulator for a pure flight management problem, assuming that the aircraft has the whole airspace for itself. Given an individual single flight, thousands of 4D trajectory variants were flown in an accurately simulated environment, until the lowest costs and risks solution is found.

During the simulated flight, the model is integrated by a 4th order Runge-Kutta method, with a time step of 1 second. The time step has to be constant, since each flight is integrated independently, and the relative distance between each aircraft pair must be calculated at each time step, to assess the loss of separation risk. Experiments with time steps ranging from 0.1 s to 10 s were made, comparing the calculated 4D trajectory with the corresponding real one based on DFDR data. For time steps larger than 3 s, distortions become significant.

The optimization algorithm is genetic, using the TCR objective function as the fitness index. All other known optimization algorithms [19] were attempted and failed, confirming the findings of other authors [20], [21]. The computing is easily parallelizable, since at every new generation of trajectories, a population of new trajectories are

flown and evaluated independently. However, for complex problems with more aircraft, parallelization in a processor cluster is possible only by flying each aircraft on an individual processor, and thus an application server may calculate all separations at each time step, after the slowest processor ended the computing sequence for that particular time step. In such a configuration, more processor clusters would be needed to evaluate more solutions in parallel.
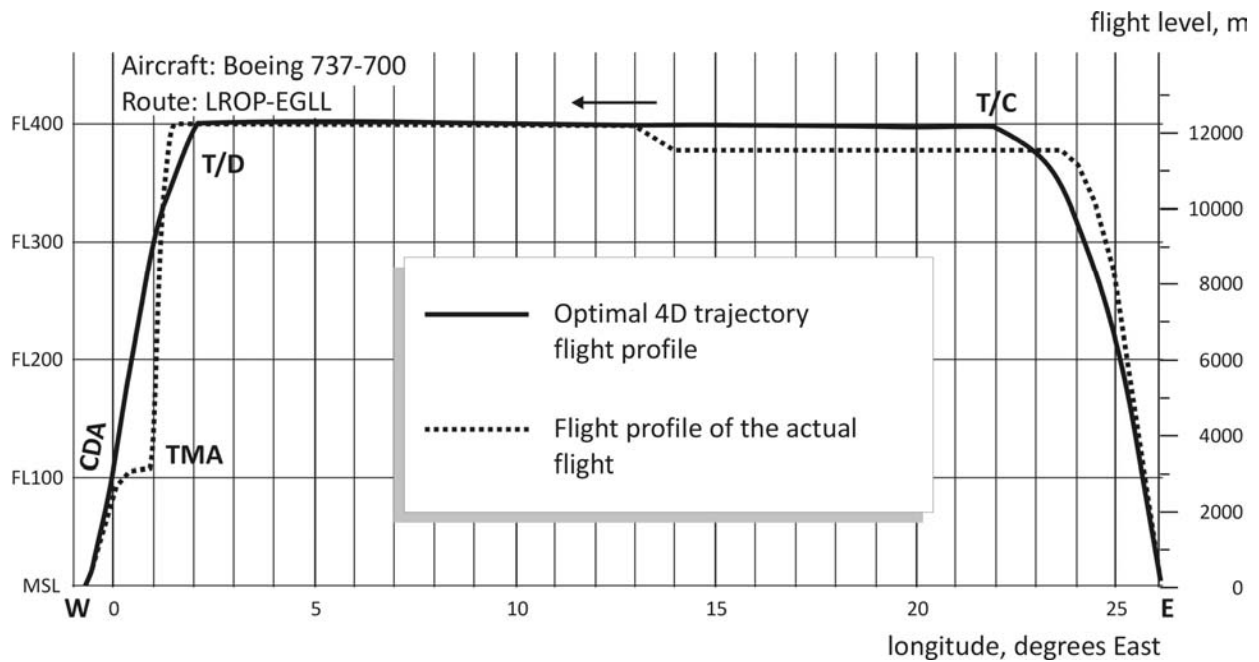
Figure 11. The optimized profile, compared to the actual flight profile.

The results of the optimization of the selected flight are presented in Figures 10 and 11. Using the best climb, cruise, and descent, and the best winds, our optimized trajectory saved 24% of fuel, compared to the orthodrome, or 16% compared to the actual flight. This was accomplished after 62 generations, and 1,860 calculated trajectories. The TCR index went down from €8,904 to €5,964, out of which the fuel cost alone decreased from €5,772 to €4,392 (Table 6). The factors contributing to the fuel savings in the optimized solution with respect to the actual flight (902 kg) are as follows: a) the continuous descent approach (CDA) accounts for 40% of the savings; the real aircraft did a very steep descent using speed brakes, as required by the ATC (see the dotted line in Figure 11), then it had to level for the deceleration to meet the speed restriction of 250 knots in the TMA b) a holding pattern in the actual flight, required for ATC sequencing purposes, skipped in the optimized one, accounts for another 15%; c) the rest of 45% of the savings are due to the better use of the wind vectors, and the constant flight level FL400. The real aircraft had to maintain FL380 half of its way, due to traffic (see the dotted line in the right section in Figure 11). Figure 12

illustrates the field of search for the optimization algorithm, superimposing all the individual trajectories attempted in the process.

Future research will focus on testing the objective function for simultaneous optimization of the 4D trajectories of more aircraft, herewith solving air traffic management problems, with all 4D trajectories safely separated.
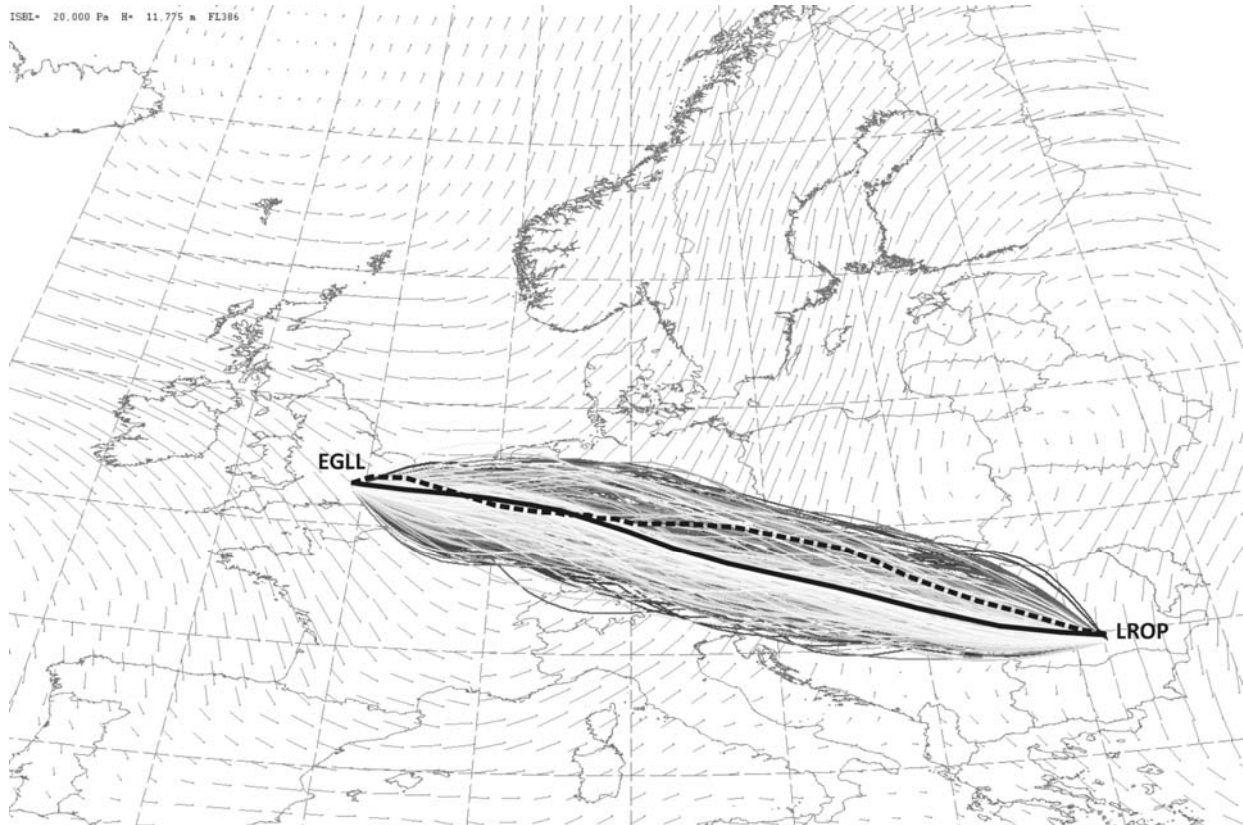
Figure 12. All routes evaluated in the optimization process.

VI.   Conclusion

As the experiments indicate, the objective function based on the total costs and risks is adequate for 4D trajectory optimization needed in a centralized TBO environment, where the trajectories required are: (a) safely separated from each other, (b) safest, with respect to risks other than separation, and (c) least expensive to fly. In the experiments with the objective function, important reductions of the total costs have resulted through the optimization process. For instance, in a 3 hours flight with a commercial airliner, fuel costs were reduced by 24%, as the case study showed.

Among other features, the objective function implements weather avoidance, no-fly zones avoidance, and wake turbulence avoidance.

The objective function presented in this paper is computationally intensive, an issue that may be addressed by parallelization and distributed computing.

For relevant results and savings with such a complex and multidisciplinary optimization, the authors found that an accurate simulation of both the aircraft and the environment is required. It was also found that, based on tests with several optimization methods, the one with genetic algorithms provided the necessary stability and convergence speed for this application.

Acknowledgments

References

[1] Bijlsma, S. J., "Optimal Aircraft Routing in General Wind Fields", *AIAA Journal of Guidance, Control and Dynamics*, Vol. 32, Number 4, May-June 2009, pp. 1025-1029.

[2] Pleter, O. T. "Simultaneous Flight and Air Traffic Management Numerical Optimization", PhD Thesis, University Politehnica of Bucharest, Faculty of Aerospace Engineering, Bucharest, Romania, Sep. 2004.

[3] Prevot, T., Shelden, S., Mercer, J., Kopardekar, P., Palmer, E., and Battiste, V., "ATM Concept Integrating Trajectory-Orientation and Airborne Separation Assistance in the Presence Of Time-Based Traffic Flow Management", *22nd Digital Avionics Systems Conference* DASC03, Indianapolis, IN, 2003.

[4] Pleter, O. T., and Ştefănescu, I. B., "Simultaneous Flight and Traffic Management System", *University Politehnica of Bucharest Scientific Bulletin*, Series D: Mechanical Engineering, Vol. 66, Number 2-4, 2004, pp. 93-104.

[5] Weber, R., Cruck, E., "Subliminal ATC Utilizing 4D Trajectory Negotiation", *Integrated Communications, Navigation and Surveillance Conference*, Volume ICNS 07, April-May 2007, pp. 1-9.

[6] Constantinescu, C. E., and Pleter, O. T., "Air Traffic Control Optimization Using Genetic Algorithms", *Proceedings, The 36-th International Scientific Simposium of METRA*, Volume II, Bucharest, Romania, 2005, pp 21-26.

[7] Clarke, J. P. et al, "En Route Traffic Optimization to Reduce Environmental Impact", *PARTNER Project 5 Report*, Massachusetts Institute of Technology, Cambridge, MA, July 2008.

[8] Granger, G., Durand, N., and Alliot, J. M., "Optimal Resolution of En Route Conflicts", *4th USA/Europe Air Traffic Management R&D Seminar* ATM-2001, 2001.

[9] Weitz, L. A., Hurtado, J. E., Bussink, F. J. L., "Increasing Runway Capacity for Continuous Descent Approaches Through Airborne Precision Spacing", *AIAA Guidance, Navigation, and Control Conference and Exhibit,* San Francisco, CA, 2005.

[10] Moldoveanu, G., and Pleter, O. T., "Multidisciplinary Optimization in Services Management", *Theoretical and Applied Economics*, Number 5, 2007, Bucharest, Romania, pp. 7-14.

[11] Pleter, O. T., Stefanescu, I. B., and Constantinescu, C. E., "Simultaneous 4D Trajectory Optimization Using Genetic Algorithms", *Proceedings of ICNPAA (International Conference on Non-linear Problems in Aviation and Aerospace)*, 2006.

[12] Pleter, O. T., and Ştefănescu, I. B., "The Baro-Geodetic Coordinate Frame in Air Navigation", *University Politehnica of Bucharest Scientific Bulletin*, Series D: Mechanical Engineering, Vol. 65, Number 1-4, 2003, pp. 155-164.

[13] Evans, M., Hastings, N., and Peacock, B., *Statistical distributions*, 3rd Edition, Wiley-Interscience, New York, 2000, Chap. 2.5.

[14] ***, "Customer Guide to Charges", *Eurocontrol*, June 2009, Version 3.5 [online publication], URL: http://www.eurocontrol.int/crco/public/subsite_homepage/homepage.html [cited 2 July 2009].

[15] ***, "Unit Rates and Tariffs", *Eurocontrol*, Central Route Charges Office [online database], URL: http://www.eurocontrol.int/crco/public/standard_page/basic_unit_rates.html [cited 2 July 2009].

[16] Pleter, O. T, and Constantinescu, C. E., "A New Approach to Optimal Air Navigation", *Proceedings, The 36-th International Scientific Simposium of METRA*, Volume II, Bucharest, Romania, 2005, pp. 77-82.

[17] Nita, M. M., Patraulea, R., and Sarbu, A. "Mecanica Aeronavelor" (in Romanian), *Institutul Politehnic Bucuresti*, Romania, 1985.

[18] ***, "Nomads: User Manual", National Climatic Data Center [online database], URL: http://nomads.ncdc.noaa.gov/guide [cited Feb 2009]

[19] Berbente, C., Pleter, O. T., and Berbente, S., "Numerische Methoden, Theorie und Anwendungen", *Editura Printech* Bucharest, Romania, 2000.

[20] Gianazza, D., "Optimisation des flux de trafic aérien", PhD Thesis, L'Institut National Polytechnique de Toulouse, Nov. 2004.

[21] Durand, N., Alech, N., Alliot, J. M., and Schoenauer, M. "Genetic Algorithms for optimal air traffic conflict resolution", *Proceedings of the Second Singapore Conference on Intelligent Systems*, SPICIS, Singapore, 1994.